

111.3
107
C. 1

TECHNICAL MEMORANDUMS
NATIONAL ADVISORY COMMITTEE FOR AERONAUTICS

No. 963

FOR REFERENCE

NOT TO BE TAKEN FROM THIS ROOM

CHORDWISE LOAD DISTRIBUTION OF A SIMPLE RECTANGULAR WING

By Karl Wieghardt

Zeitschrift für angewandte Mathematik und Mechanik
Vol. 19, No. 5, October 1939

1.2.1.1
1.9.1.

Washington
December 1940



NATIONAL ADVISORY COMMITTEE FOR AERONAUTICS

TECHNICAL MEMORANDUM NO. 963

CHORDWISE LOAD DISTRIBUTION OF
A SIMPLE RECTANGULAR WING*

By Karl Wioehardt

I. SEVERAL VORTEX FILAMENTS.

In the airfoil theory of Prandtl (reference 1) the wing is replaced by a lifting vortex filament whose circulation varies over the span. By this method the "first problem of airfoil theory," namely, for a given lift distribution to determine the shape of the airfoil, was solved. The inverse "second problem," namely, for a given wing to determine the lift distribution, was then solved by Betz (reference 2), the computation being simpler for small aspect ratios than for large ones. For the latter, an approximate solution was obtained by Trefftz (reference 3). The answer was thus found to the most important practical question, namely, the manner in which the wing forces are distributed along the span.

The chordwise distribution theory was simply taken over from the theory of the infinite wing. The Ackermann formulas, published by Birnbaum (reference 4), in which the infinite wing was replaced by a plane vortex sheet - on account of their linearized form permit also application to the finite wing and this application was carried out by Blenk (reference 5) for the rectangular wing. Since in this work a series expansion in b/t was used, the computation converges only for large aspect ratios. In the present paper a useful approximate solution will be found also for wings with large chord - i.e., small aspect ratio.

Another method of investigating the lift distribution along the two dimensions (span and chord) was found by Prandtl (reference 6) in his use of the acceleration potential. This method assumes, however, that the potential is known for a suitable number of source distribu-

*"Über die Auftriebsverteilung des einfachen Rechteckflügels über die Tiefe." Zeitschrift für angewandte Mathematik und Mechanik, vol. 19, no. 5, Oct. 1939, pp. 257-270.

tions over the horizontal projection of the wing. The first application was made by Kinner (reference 7) in his work on the wing with circular plan form, since these functions are obtainable for the circle. The method appears, however, for the present to offer no promise for the rectangular wing, since no expansion of the potential into a series of known functions is known for the rectangle. For this reason the computation in the present paper will still be conducted by the vortex-sheet method.

For accurate investigation of the lift distribution, the wing must be replaced by a vortex sheet. A good idea of the distribution can still be obtained if the wing is represented by a finite number of discrete vortex filaments, and the necessary amount of computation is thereby reduced considerably as compared with the continuous circulation distribution. This is because in the case of the vortex sheet, the condition that the component of the induced velocity at right angles to the wing should be equal to that due to the flow, gives rise to an integral equation. For individual vortex filaments, however, this flow condition need be satisfied exactly only at single points, so that only a system of linear equations is obtained. Figure 1 shows such a vortex system, for which the computation was carried out. In order that the results obtained from using only a few vortices, or even a single one, be as accurate as possible, the distance of the first vortex filament from the leading edge is taken to be $a/4$. It is known from previous work that the circulation in the neighborhood of the leading edge increases as $1/\sqrt{x}$; the foremost, strongest vortex which gives the circulation contribution from the leading edge to the foremost points considered, then lies exactly at the center of pressure of the forward lift portion because the center of gravity of $y = c/\sqrt{x}$ lies at $s = x/3$. The points at which the total velocity at right angles to the wing is made to vanish, lie in the center between two vortex lines and at $x = t = a/4$. The wing is a plane rectangular plate of zero thickness with chord $t = na$ for n vortices. The notation is indicated in figure 1. The coordinates of the point A are x^* and y^* . The velocity at right angles to the xy plane, induced by the bound and trailing vortices at the point A, is then given by the Biot-Savart law:

$$w_A = \sum_1^n \left\{ \frac{\bar{x}_1}{4\pi} \int_{-b/2}^{+b/2} \frac{\Gamma_1(y) dy}{[\bar{x}_1^2 + (y - y^*)^2]^{3/2}} \right. \\ \left. - \frac{\bar{x}_1}{4\pi} \int_{-b/2}^{+b/2} \frac{\frac{d\Gamma_1(y)}{dy}}{\sqrt{\bar{x}_1^2 + (y - y^*)^2}} \frac{dy}{y - y^*} \right. \\ \left. - \frac{1}{4\pi} \int_{-b/2}^{+b/2} \frac{1}{y - y^*} \frac{d\Gamma(y)}{dy} dy \right\} \quad \bar{x}_1 = x^* - x_1 \quad (1)$$

The first integral, which arises from the bound vortices, gives after integration by parts:

$$\left[\frac{(y - y^*) \Gamma_1(y)}{\bar{x}_1^2 \sqrt{\bar{x}_1^2 + (y - y^*)^2}} \right]_{-b/2}^{+b/2} \\ - \int_{-b/2}^{+b/2} \frac{(y - y^*)}{\bar{x}_1^2 \sqrt{\bar{x}_1^2 + (y - y^*)^2}} \frac{d\Gamma_1(y)}{dy} dy$$

The first expression vanishes since the circulation at the tips must be zero; $\Gamma(\pm \frac{b}{2}) = 0$. There is thus obtained "A":

$$w_A = - \frac{1}{4\pi} \sum_1^n \int_{-b/2}^{+b/2} \frac{d\Gamma_1(y)}{dy} \frac{1}{y - y^*} \left(1 + \frac{\sqrt{\bar{x}_1^2 + (y - y^*)^2}}{\bar{x}_1} \right) dy \quad (1a)$$

Since $\Gamma_1(y)$ decreases from the center of the plate toward the tips, $\frac{d\Gamma_1(y)}{dy} < 0$, and hence $w_A > 0$. From the condition $W_A = V \sin \alpha$, there are obtained for n points n equations $w_{A_1} = w_{A_2} = \dots = w_{A_n} = V \sin \alpha$. It is thus possible either to assume the same spanwise circulation distribution - for example, the elliptic for all $n = m$ vortices - or set up a series expansion with r undetermined coefficients for $n = m/r$ vortices.

An example by the second method will first be computed. For this purpose, the following transformation of coordinates is made:

$$y = \frac{b}{2} \cos \varphi, y^* = \frac{b}{2} \cos \varphi^*; \quad \bar{x}_1 = x^* - x_1 = \frac{b}{2} \delta_1$$

so that $-\frac{b}{2} \leq y \leq \frac{b}{2}$ corresponds to $\pi \geq \varphi \geq 0$. Equation (1a) then becomes:

$$w_A = \frac{1}{2\pi b} \sum_{i=1}^n \int_0^\pi \frac{1}{\cos \varphi - \cos \varphi^*} \left(1 + \frac{\sqrt{\delta_1^2 + (\cos \varphi - \cos \varphi^*)^2}}{\delta_1} \right) \frac{d\Gamma_1(\varphi)}{d\varphi} d\varphi \quad (2)$$

For each $\Gamma_1(\varphi)$, a trigonometric series that contains only the $\sin(2v+1)\varphi$ terms was assumed, since the relations are assumed symmetric with respect to the wing center: $\Gamma_1(\varphi) = \Gamma_1 \sin \varphi (1 + a_1^{(1)} \sin \varphi + a_1^{(2)} \sin 3\varphi)$. Thus for each vortex filament, there are three undetermined coefficients Γ_1 , $a_1^{(1)}$, and $a_1^{(2)}$. We then have

$$\begin{aligned} \frac{d\Gamma_1(\varphi)}{d\varphi} = & \Gamma_1 (\cos \varphi + 2a_1^{(1)} \sin \varphi \cos \varphi \\ & + a_1^{(2)} \cos \varphi \sin 3\varphi + 3a_1^{(2)} \sin \varphi \cos 3\varphi) \end{aligned}$$

Substituting this expression in equation (2), there is obtained:

$$w_A = - \frac{1}{2\pi b} \sum_1^n \Gamma_1 \left\{ \frac{1}{\delta \delta_1} J - \pi + a_1^{(1)} f_1(\delta_1, \cos \varphi^*) + a_1^{(2)} f_2(\delta_1, \cos \varphi^*) \right\} \quad (3)$$

where the functions f_1 and f_2 are made up of integrals which may be evaluated by elementary methods. The integral J , which is also a function of δ_1 and $\cos \varphi^*$ is, in any particular case to be determined by graphical or numerical methods. The integral is

$$J = \int_0^\pi \frac{\cos \varphi \, d\varphi}{\cos \varphi - \cos \varphi^*} \sqrt{\delta_1^2 + (\cos \varphi - \cos \varphi^*)^2} =$$

$$= \int_0^\pi \frac{(\cos \varphi - \cos \varphi^*)}{\delta_1^2 + \sqrt{\delta_1^2 + (\cos \varphi - \cos \varphi^*)^2}} \cos \varphi \, d\varphi + \pi \delta_1$$

for δ_1 and $\cos^* > 0$. Through this transformation the singularity at $\varphi \rightarrow \varphi^*$ has been removed. Since for each vortex line there are three undetermined coefficients, the flow condition can be satisfied for each set of three points between two lines and for three points at $x = t - a/4$. On account of the symmetry $3n$, different points may be chosen on a half wing and for the corresponding points, symmetrical with respect to the center line of the plate, the condition $w_A = V \sin \alpha$ is then automatically satisfied. Altogether, therefore, the flow condition is accurately satisfied for $6n$ points or, in case one of each set of three points lies on the center line, for $5n$ points. The entire computation is based on the expectation that the condition $w_A = V \sin \alpha$ will be, on the average, satisfied at least approximately, also at other points of the surface, and that the singular behavior of w_A along each of the lifting vortices will not have too great an effect on the approximate computation of the circulation. Although aerodynamically this can only be justified by considering the plate as replaced by several wings lying one behind the other, each represented by a

vortex filament. The choice of the number of vortex filaments n is, for practical reasons, restricted since while the number of points considered increases only linearly with n , the required computation work of solving the system of $3n$ equations increases at a greater rate.

The numerical computation was carried out for the following case: $n = 4$, $\varphi^* = 30^\circ (150^\circ)$, $60^\circ (120^\circ)$, and 90° (center line) with $b = 4a$, corresponding to an aspect ratio of $A = b/t = 1$. (See fig. 2.) The integral J ($J(+\delta_1) = J(-\delta_1)$) was determined for the four values $1/4, 3/4, 5/4, 7/4$ which are assumed by δ_1 and, on account of the symmetry, for only three values of COB φ^* . For $\varphi^* = 90^\circ$, an elliptic integral of the second kind is obtained for J . From the functions $f_1(\delta_1, \cos \varphi^*)$ and $f_2(\delta_1, \cos \varphi^*)$, the coefficients were obtained for a system of 12 equations which was solved by the usual elimination process with the computation machines since the system could not be solved by iteration. As the computation was carried out to only five decimal places, it was afterwards found to be of insufficient accuracy for the determination of the last three unknowns; the circulation of the rear-most vortex filament, therefore, could only be estimated by extrapolation. For the remaining circulations, there was obtained:

$$\begin{aligned} \Gamma_1 &= +0.737_0 bV \sin \alpha & \Gamma_2 &= +0.116_2 bV \sin \alpha & \Gamma_3 &= +0.058_4 bV \sin \alpha \\ a_1^{(1)} &= -0.136_3 & a_2^{(1)} &= +0.564_2 & a_3^{(1)} &= +0.245_5 \\ a_1^{(2)} &= +0.005_7 & a_2^{(2)} &= +0.001_2 & a_3^{(2)} &= -0.061_1 \end{aligned}$$

Those circulation distributions are shown on figure 3.

Integrating over the span:

$$\rho V \frac{b}{2} \int_0^\pi \Gamma_1(\varphi) \sin \varphi d\varphi = \rho V \frac{b}{2} \Gamma_1 \left(\frac{\pi}{2} + \frac{4}{3} a_1^{(1)} - \frac{4}{15} a_1^{(2)} \right)$$

these may be considered by the Kutta-Joukowski theorem as the lift contributions of the individual wing strips (along the chord). The lift is then distributed as follows:

From the leading edge to $3t/16$: $A_I = -0.512$, $\rho b t V^2 \sin \alpha$
 From $3t/16$ to $7t/16$: $A_{II} = 0.133$, "
 From $7t/16$ to $11t/16$: $A_{III} = 0.055$, "
 From $11t/16$ to trailing edge $A_{IV} \approx 0.02$, "

The total lift is $A = \sum A_\mu = 0.72s \rho b t V^2 \sin \alpha$ and the lift coefficient $c_a = A / \frac{\rho}{2} b t V^2 = 1.44 \sin \alpha$. The moment about the leading edge is obtained as the sum of the moments of the several strips: $M = t/16 (A_I + 5A_{II} + 9A_{III} + 13A_{IV})$ and the moment coefficient $c_m = 0.243 \sin \alpha$. The position of the center of pressure is obtained from $s = \frac{c_m}{c_a} t = 0.16 t$, where s is the distance of the center of pressure from the leading edge. Finally, for the

forward three vortices the factor $v_1 = \frac{\int_0^\pi \Gamma_1(\varphi) \sin \varphi d\varphi}{2(1+a_1)(1-a_1)}$ can be determined: $v_1 = 0.809$, $v_2 = 0.74$, $v_3 = 0.73$.

Since for all vortices this factor is approximately equal to $\pi/4 = 0.7854$, it appears justifiable - at least, for deep wings, that is, small aspect ratios $A = b/2$ - to assume initially an elliptic spanwise lift distribution and so considerably simplify the computation. The fact that this assumption, according to the above computed example, is not quite applicable to the rear vortices, is of no great importance on account of the strong rearward drop in the circulation,

Since for elliptic distribution there is only one undetermined coefficient for each vortex line, namely, the circulation Γ_i in the center of the span, the flow condition $w_A = V \sin \alpha$ can also be satisfied at only one point (and the point symmetrical with respect to the center line) between each two lines and at $x = 15t/16$. For this reason, the assumed points are taken on the center line and in the center between each two succeeding lines, and the last at $x = 15t/16$. We then have $y^* = 0$, $x^* = \frac{1}{2} (x_k + x_{k+1})$.

for the rearmost point $x^* = 15t/16$ and $\bar{x}_1 = \pm \frac{t}{2n}, \pm \frac{at}{2n}, \dots + \frac{2(n-1)t}{2n}$, where n is the number of vortices. Substituting $\Gamma_1(y) = \Gamma_1 \sqrt{1 - \left(\frac{y}{b/2}\right)^2}$, $\frac{d\Gamma_1(y)}{dy} = - \frac{\Gamma_1 y}{\left(\frac{b}{2}\right)^2 \sqrt{1 - \left(\frac{y}{b/2}\right)^2}}$

into equation (1a), there is obtained for the induced velocity at the point considered:

$$w_A = \frac{1}{\pi b^2} \sum_1^n \Gamma_1 \int_{-b/2}^{+b/2} \frac{1}{\sqrt{1 - \left(\frac{y}{b/2}\right)^2}} \left(1 + \frac{\sqrt{\bar{x}_1^2 + y^2}}{\bar{x}_1} \right) dy$$

$$= \frac{1}{\pi b^2} \sum_1^n \Gamma_1 \left\{ \pi \frac{b}{2} + \frac{2}{\bar{x}_1} \int_{-b/2}^{+b/2} \sqrt{\frac{\bar{x}_1^2 + y^2}{1 - \left(\frac{y}{b/2}\right)^2}} dy \right\}$$

The elliptic second integral is reduced to the normal form by the substitution $y = b/2 \cos \psi$, so that there is obtained:

$$w_A = \frac{1}{\pi b} \sum_1^n \Gamma_1 \left\{ \frac{\pi}{2} + \frac{\sqrt{\bar{x}_1^2 + (b/2)^2}}{\bar{x}_1} E \left(\frac{b/2}{\sqrt{\bar{x}_1^2 + (b/2)^2}}, \frac{\pi}{2} \right) \right\} \quad (4)$$

where E is the complete elliptic integral of the second

$$\text{kind } E \left(k, \frac{\pi}{2} \right) = \int_0^{\pi/2} \sqrt{1 - k^2 \sin^2 \psi} d\psi \text{ with modulus } k =$$

$$\frac{b/2}{\sqrt{\bar{x}_1^2 + (b/2)^2}}. \text{ This function is tabulated, for example,}$$

in Jahnske-Emde: Funktionentafeln. It has the following limiting value for $k = \sin \varphi$, $0 \leq k \leq 1$, $0 \leq \varphi \leq \pi/2$, and in the above equation for $\infty \geq |\bar{x}_1| \geq 0$: $\frac{\pi}{2} \geq E \left(\varphi, \frac{\pi}{2} \right) \geq 1$.

The expression in parentheses in equation (4) gives the coefficients for the linear nonhomogeneous system of equations for the n unknowns $\Gamma_1, \Gamma_2, \dots, \Gamma_n$. Putting $2b$ on the right side, it reads $2b V \sin \alpha$ for all equations, on account of the condition $w_A = V \sin \alpha$. The coefficients of the principal diagonal are all equal and similarly in each diagonal from upper left to lower right. Thus, for example, for $\lambda = 6$, $n = 4$; that is, $\bar{x}_1 = \pm b/40$,

- $3b/48, \pm 5b/48, \pm 7b/48$, the system becomes:

$$\begin{aligned} 16.346_1 \Gamma_1 - 14.346_1 \Gamma_2 - 4.250_3 \Gamma_3 - 2.284_2 \Gamma_4 &= 2b V \sin \alpha \\ 6.250_3 \Gamma_1 + 16.346_1 \Gamma_2 - 14.346_1 \Gamma_3 - 4.250_3 \Gamma_4 &= 2b V \sin \alpha \\ 4.284_2 \Gamma_1 + 6.250_3 \Gamma_2 + 16.346_1 \Gamma_3 - 14.346_1 \Gamma_4 &= 2b V \sin \alpha \\ 3.470_4 \Gamma_1 + 4.284_2 \Gamma_2 + 6.250_3 \Gamma_3 + 16.346_1 \Gamma_4 &= 2b V \sin \alpha \end{aligned}$$

with the solutions

$$\Gamma_1 = 1.334_4 t V \sin \alpha \quad \Gamma_3 = 0.328_0 t V \sin \alpha$$

$$\Gamma_2 = 0.558_3 t V \sin \alpha \quad \Gamma_4 = 0.179_1 t V \sin \alpha$$

The lift contributions from the four strips of the wing are: $A_I = 1.048, b t v \sin \alpha$, $A_{II} = 0.478_5 b t V \sin \alpha$, $A_{III} = 0.257_8 b t V \sin \alpha$, $A_{IV} = 0.143, b t V \sin \alpha$; the coefficients: $c_a = 3.76_8 \sin \alpha$, $c_w = 0.754 \sin^2 \alpha$, $c_m = 0.92_3 \sin \alpha$, and the distance of the center of pressure from the leading edge $s = 0.24, t$. A comparison of the results by this method and those by the Vortex-surface method will be made in the third section.

Still simpler is the limiting case of the above system for $n = 1$. The computation is then made with a vortex with spanwise elliptic circulation distribution at the distance $t/4$ from the leading edge. The single point considered lies at $x = 3/4 t$. The center of pressure, according to the assumption then, always lies at $s = t/4$, which is sufficiently accurate for rather large aspect ratios $\lambda > 3$, as shown by the computation with the vortex sheet. The circulation and the coefficients in this case can, in general, be explicitly expressed:

$$\Gamma = \frac{2b V \sin \alpha}{1 + \frac{2}{\pi} \sqrt{1 + \lambda^2} E\left(\frac{\lambda}{\sqrt{1 + \lambda^2}}, \frac{\pi}{2}\right)};$$

$$c_a = \frac{\pi \lambda \sin \alpha}{1 + \frac{2}{\pi} \sqrt{1 + \lambda^2} E\left(\frac{\lambda}{\sqrt{1 + \lambda^2}}, \frac{\pi}{2}\right)}, c_{w1} = \frac{1}{\pi \lambda} c_a^2, c_{w4} = \frac{1}{4} c_a$$

With infinitely increasing aspect ratio there is thus obtained a limiting value for c_a : $\lim_{\lambda \rightarrow \infty} c_a = \frac{\pi^2}{2} \sin \alpha$. From the potential theory, on the other hand, there is obtained for the wing with infinite span $c_a = 2\pi \sin \alpha$. This difference is readily explainable from the fact that elliptic circulation distribution (that is, factor 7, previously defined, equals $n/4$) has been assumed above. According to Betz, however, this factor for rectangular wings becomes larger with increasing λ up to the limiting value 1 for $\lambda \rightarrow \infty$. Hence, multiplying by $4/\pi$, we have actually $\frac{4}{\pi} \lim_{\lambda \rightarrow \infty} c_a = (c_a)_{\text{pot}}$.

It is now simple to refine this method by assuming a trigonometric series for $\Gamma(x): y = \frac{b}{2} \cos \varphi$, $\Gamma(\varphi) = \Gamma \sin \varphi (1 + a_1 \sin \varphi + \dots + a_n \sin n \varphi)$. Then, again, equation (3) is obtained - this time for one vortex with $\delta_1 = 1/\lambda$; that is, without the summation sign. The drag is determined

$$\text{from } W = \rho \frac{b}{2} \int_0^\pi \Gamma(\varphi) w(\varphi) \sin \varphi d\varphi, \text{ where } w(\varphi) = \frac{1}{2\pi b} \int_0^\pi \frac{1}{\cos \varphi - \cos \varphi'} \frac{d\Gamma(\varphi')}{d\varphi'} d\varphi', \text{ and there is obtained } c_{w1} = \left(\frac{\pi}{2} + \frac{4}{3} a_1 + \frac{2}{\pi} a_1^2 + \dots + \frac{\Gamma^2}{V^2 b t}\right).$$

In the examples there was set: $\Gamma(\varphi) = \Gamma \sin \varphi (1 + a_1 \sin \varphi)$, $\varphi_1^* = 30^\circ$, $\varphi_2^* = 60^\circ$, which corresponds to $y_1^* = \frac{\sqrt{3}}{4} b$, $y_2^* = \frac{b}{4}$. On figure 4 the lift-distribution coefficient is plotted against the

aspect-ratio. It may be seen that the experimentally obtained lift coefficients (reference 8) are very closely approached by this simple amputation.

The following table is to be used in connection with figure 4:

λ	C_L	C_W	C_m	γ
$\rightarrow 0$	$\rightarrow \frac{\pi}{2} \lambda \sin \alpha$	$\rightarrow \frac{\pi}{4} \lambda \sin^2 \alpha$	$\rightarrow \frac{\pi}{8} \lambda \sin \alpha$	$\rightarrow \frac{\pi}{4}$
4/7	0.89 ₆ sin α	0.41 ₇ sin ² α	0.22 ₄ sin α	0.785 ₇
4/3	1.81 ₄ sin α	0.78 ₈ sin ² α	0.45 ₄ sin α	0.788 ₉
6	4.202 ₂ sin α	0.93 ₂ sin ² α	1.05 ₁ sin α	0.838 ₇

II. VORTEX SHEET

With the method of discrete vortex filaments, a further refinement in the lift distribution - hence an increase in the accuracy by increasing the number of vortices - is practically excluded on account of the computation labor involved. It was therefore carried to the limit $n \rightarrow \infty$, and an attempt was made by analytical methods to restrict the computation work as far as possible. On increasing n , the circulation contributed by each of the vortices and their distances apart become smaller up to the limiting case $n \rightarrow \infty$, when the circulation distribution becomes a surface distribution. The dimensions of this surface distribution $\gamma(x,y)$ are circulation per unit chord, that is, centimeters per second. An infinitesimal vortex $\gamma(x,y) dx$ induces, according to equation (1), at any point of the surface, the velocity:

$$+b/2$$

$$dw_A = \frac{1}{4\pi} \int_{-b/2}^{+b/2} \frac{(x^*-x) \gamma(x,y) dx}{[(x^*-x)^2 + (y-y^*)^2]^{3/2}} dy$$

$$= \frac{1}{4\pi} \int_{-b/2}^{+b/2} \frac{1}{y-y^*} \frac{\partial \gamma(x,y)}{\partial x} dx \left[1 + \frac{x^*-x}{\sqrt{(x^*-x)^2 + (y-y^*)^2}} \right] dy$$

where α is assumed small enough so that $\sin^2 \alpha \approx 0$ and $\cos \alpha \approx 1$. The equation would be strictly true if the trailing vortices were shed in the direction of the wing. Integrating the first integral by parts, there is again obtained, on account of $\gamma(x, y = \pm b/2) = 0$,

$$w_A = -\frac{1}{4\pi} \int_0^t dx \int_{-b/2}^{+b/2} \left\{ \frac{\sqrt{(x^*-x)^2 + (y-y^*)^2}}{(x^*-x)(y-y^*)} + \frac{1}{y-y^*} \right\} \frac{\partial \gamma(x, y)}{\partial y} dy$$

The condition $w_A = V \sin \alpha$ gives, after a transformation of coordinates,

$$\begin{aligned} x &= t/2(1 + \xi) \\ y &= b/2 \eta \end{aligned} \quad - \int_{-1}^{+1} \int_{-1}^{+1} \left\{ \frac{\sqrt{(\xi^* - \xi)^2 + \lambda^2 (\eta - \eta^*)^2}}{(\xi^* - \xi)(\eta - \eta^*)} + \frac{1}{\eta - \eta^*} \right\} \frac{\partial \gamma(\xi, \eta)}{\partial \eta} d\xi d\eta = 4\pi A V \sin \alpha \quad (5)$$

This is a two-dimensional linear integral equation of the first kind $\frac{\partial \gamma(\xi, \eta)}{\partial \eta}$. On account of the singularity of the kernel at the point considered for $\xi \rightarrow \xi^*$, $\eta \rightarrow \eta^*$, this

equation could not be solved even approximately since the usual method of approximating the kernel by a polynomial, assumes continuity. Also the particular property of the kernel on which it depends $(\xi - \xi^*)$ and $(\eta - \eta^*)$ could not be used for a solution method.

The only recourse therefore is to simplify the integral equation by an aerodynamically reasonable assumption. It was thus assumed that the spanwise circulation distribution is the same for all ξ . This results in a lowering of the order of the integral equation. Although the flow condition can then no longer be satisfied over the entire wing but only on a straight line $\eta^* = \text{const.}$ For obvious reasons elliptic distribution was assumed over the span. and $\eta^* = 0$; that is, the flow condition was to be satisfied on the center line of the plate. For these points of the surface then, the condition $v_A = V \sin \alpha$ is required,

and for other points it is expected that the deviation from this condition is not too large.

$$\text{With } \gamma(\xi, \eta) = \gamma(\xi) \sqrt{1 - \eta^2}, \quad \frac{\partial \gamma(\xi, \eta)}{\partial \eta} = - \frac{\eta}{\sqrt{1 - \eta^2}} \gamma(\xi)$$

and $\eta^* = 0$, equation (5) simplifies to the following:

$$\int_{-1}^{+1} \gamma(\xi) d\xi \int_{-1}^{+1} \left\{ \frac{\sqrt{(\xi^* - \xi)^2 + \lambda^2 \eta^2}}{(\xi^* - \xi)\eta} + \frac{1}{\eta} \right\} \frac{\eta}{\sqrt{1 - \eta^2}} d\eta = 4\pi \lambda V \sin \alpha$$

In the integration with respect to η , on elliptic integral is again obtained:

$$\int_{-1}^{+1} \frac{\sqrt{(\xi^* - \xi)^2 + \lambda^2 \eta^2}}{(\xi^* - \xi) \sqrt{1 - \eta^2}} d\eta = 2 \sqrt{1 + \frac{\lambda^2}{(\xi^* - \xi)^2}} \int_0^{\pi/2} \sqrt{1 - \frac{\lambda^2}{\lambda^2 + (\xi^* - \xi)^2} \sin^2 \varphi} d\varphi,$$

with $\eta = \cos \varphi$, so that

$$\int_{-1}^{+1} \left\{ \frac{\sqrt{(\xi^* - \xi)^2 + \lambda^2}}{(\xi^* - \xi)} E \left(\frac{\lambda}{\sqrt{\lambda^2 + (\xi^* - \xi)^2}}, \frac{\pi}{2} \right) + \frac{\pi}{2} \right\} \gamma(\xi) d\xi = 2\pi \lambda V \sin \alpha^{**} \quad (6)$$

*Corresponding integral equations can also be set up for airfoils with arbitrary plan form symmetrical with respect to the center line. If $b(\xi)$ is the span, varying with the chord, equation (5) becomes:

$$\lambda(\xi) = \frac{b(\xi)}{c}: \int_{-1}^{+1} \int_{-1}^{+1} \left\{ \frac{\sqrt{(\xi^* - \xi)^2 + \lambda^2 (\xi)(\eta - \eta^*)^2}}{(\xi^* - \xi)(\eta - \eta^*)} + \frac{1}{\eta - \eta^*} \right\} \frac{\partial \gamma(\xi, \eta)}{\partial \eta} \frac{1}{\lambda(\xi)} d\xi d\eta = 4\pi V \sin \alpha$$

(Continued on p. 14)

Equation (5) is thus reduced to a one-dimensional integral equation. The kernel, it is true, has become more complicated, and the singularity for $\xi \rightarrow \xi^*$ naturally, still remains. For the approximate solution of this equation, there is assumed for $\gamma(\xi)$ a series of functions which Birnbaum has used in his paper

$$\gamma(\xi) = A_1 \sqrt{\frac{1-\xi}{1+\xi}} + A_2 \sqrt{1-\xi^2} + A_3 \xi \sqrt{1-\xi^2} + A_4 \xi^2 \sqrt{1-\xi^2} \quad (7)$$

The four undetermined coefficients A_1, A_2, A_3, A_4 are so determined that the integral equation is satisfied at four points ξ_1 to ξ_4 . Since the kernel contains λ , it is necessary to compute each time for a definite aspect ratio. The integrations, on account of the complicated kernel, must be carried out graphically or numerically. The procedure of the very laborious computation thus, is the following:

The four basic functions $\gamma_1, \gamma_2, \gamma_3$, and γ_4 for a series of values of ξ from -1 to +1, are first computed; then for the same arguments for a definite A , the kernel functions $k(\lambda; \xi^*, \xi)$ for the four points considered. (In the examples carried out $\xi_1^* = -\frac{1}{2}, \xi_1 = 0, \xi_3^* = +\frac{1}{2}, \xi_4^* = +1$; then, on account of $k(-\xi^*, -\xi) = k(\xi^*, \xi) + \pi$, $k(-0.5, \xi) = k(+0.5, \xi) + \pi$.) Each of these kernel functions is multiplied by $\gamma_1(\xi), \gamma_2(\xi), \gamma_3(\xi), \gamma_4(\xi)$:

** (Continued from p. 13)

For the elliptic wing there is obtained for elliptic circulation distribution over the span with $\lambda(\xi) = b_{\max}/t \sqrt{1-\xi^2}$:

$$\int_{-1}^{+1} \left\{ \frac{\sqrt{(\xi^* - \xi)^2 + \lambda^2 (1 - \xi^2)}}{(\xi^* - \xi)} \mp \left(\frac{\lambda \sqrt{1 - \xi^2}}{\sqrt{\lambda^2 (1 - \xi^2) + (\xi^* - \xi)^2}}, \frac{\pi}{2} \right) + \frac{\pi}{2} \right\} \frac{\gamma(\xi)}{\lambda \sqrt{1 - \xi^2}} d\xi = 2\pi V \sin \alpha; \quad \lambda = \frac{b_{\max}}{t}$$

This equation is solved approximately as in the case of the rectangular wing. The limiting case $A \rightarrow \infty$ gives for

$$\frac{1}{2\pi} \int_{-1}^{+1} \frac{1}{\xi^* - \xi} \gamma(\xi) d\xi = V \sin \alpha \quad \text{the solution of the potential theory } \gamma(\xi) = 2V \sin \alpha \frac{1-\xi}{1+\xi} \quad \text{with } c_a = 2\pi \sin \alpha, \quad c_n = \frac{\pi}{2} \sin \alpha, \quad s = \frac{1}{4} t.$$

$$\begin{aligned}
 i_1(\xi) &= k(\xi_1^*, \xi) \gamma_1(\xi) & i_5(\xi) &= k(\xi_5^*, \xi) \gamma_5(\xi) \\
 i_2(\xi) &= k(\xi_1^*, \xi) \gamma_2(\xi) & i_6(\xi) &= k(\xi_2^*, \xi) \gamma_2(\xi) \\
 i_3(\xi) &= k(\xi_1^*, \xi) \gamma_3(\xi) \\
 i_4(\xi) &= k(\xi_1^*, \xi) \gamma_4(\xi) \\
 &\text{etc. to} \\
 i_{16}(\xi) &= k(\xi_4^*, \xi) \gamma_4(\xi)
 \end{aligned}$$

These 16 functions must now be integrated graphically or numerically: for example, by the Simpson rule:

$$I_k = \int_{-1}^{+1} i_k(\xi) d\xi$$

Since the $k(\xi^*, \xi)$ and hence the $i(\xi)$ become infinite for $\xi \rightarrow \xi^*$, it is necessary in the quadrature to exclude a region $\xi^* - \epsilon < \xi < \xi^* + \epsilon$ and approximately determine by analytical methods the Cauchy principal value

$\int_{\xi-\epsilon}^{\xi+\epsilon} i(\xi) d\xi$. We thus finally have the coefficients

I_k for the linear nonhomogeneous system of equations:

$$\sum_{v=1}^4 I_{4\mu+v} A_v = 2\pi \lambda v \sin \alpha \quad \text{for } \mu = 0, 1, 2, 3, \dots$$

from which the $A_v(\lambda)$ can be determined. We then have:

$\gamma(\lambda; \xi, \eta) = \sum_{v=1}^4 A_v(\lambda) \gamma_v(\xi) \sqrt{1 - \eta^2}$. In this manner the circulation distribution was determined for the aspect ratios $A = 1/4, 1/2$, and 1.

For greater aspect ratios, $A > 2$, the 16 graphical quadratures are not required, but the approximate computation can be carried out analytically. For this purpose the elliptic integral must approximately be evaluated for $45^\circ < \varphi \leq 90^\circ$. Since $\sin \varphi = \frac{\lambda}{\sqrt{\lambda^2 + (\xi^* - \xi)^2}}$ and $|\xi^* - \xi| \leq 2$,

$\varphi = 45^\circ$ is the smallest argument for $\lambda \geq 2$. For this range $E(x, \pi/2)$ was replaced by $\bar{E}(x, \pi/2) = 1 + 0.44 \sqrt{1-x^2}$. At first there was set $E(x, \pi/2) = 1 + \left(\frac{\pi}{2} - 1\right) \sqrt{1-x^2} \sum_0^{\pi} v a_v x^v$, but the computation then became so complicated that there was no advantage gained over the previous method; E is thus determined with an error which is approximately -3 percent for $\varphi = 45^\circ$, +3.6 percent (maximum value) for $\varphi = 80^\circ$, and approaches zero as $\varphi \rightarrow 90^\circ$. For $\varphi = 90^\circ$, the first derivatives also

agree: $\lim_{x \rightarrow 1} \frac{d\bar{E}(x, \frac{\pi}{2})}{dx} \rightarrow -\infty$ and

$$\lim_{x \rightarrow 1} \frac{dE(x, \frac{\pi}{2})}{dx} = \lim_{x \rightarrow 1} \int_0^{\pi/2} \frac{-x \sin \varphi}{\sqrt{1-x^2 \sin^2 \varphi}} d\varphi \rightarrow -\infty$$

For $\lambda > 2$ the radical can be developed into a power series which converges for all ξ^* , since $|\xi^* - \xi| \leq 2$. With

$$E\left(\frac{\lambda}{\sqrt{\lambda^2 + (\xi^* - \xi)^2}}, \frac{\pi}{2}\right) \approx \bar{E}\left(\frac{\lambda}{\sqrt{\lambda^2 + (\xi^* - \xi)^2}}, \frac{\pi}{2}\right) =$$

and

$$1 + 0.44 \frac{|\xi^* - \xi|}{\sqrt{\lambda^2 + (\xi^* - \xi)^2}}$$

and

$$\sqrt{\lambda^2 + (\xi^* - \xi)^2} \approx \lambda \left[1 + \frac{1}{2} \left(\frac{\xi^* - \xi}{\lambda}\right)^2 - \frac{1}{8} \left(\frac{\xi^* - \xi}{\lambda}\right)^4 + \frac{1}{16} \left(\frac{\xi^* - \xi}{\lambda}\right)^6 \right]$$

equation (6) then becomes:

$$\begin{aligned} & \int_{-1}^{+1} \left\{ \frac{\lambda}{\xi^* - \xi} + \frac{1}{2\lambda} (\xi^* - \xi) - \frac{1}{8\lambda^3} (\xi^* - \xi)^3 + \frac{1}{16\lambda^5} (\xi^* - \xi)^5 \right\} \gamma(\xi) d\xi \\ & + \int_{-1}^{+1} \left(0.44 \operatorname{sign}(\xi^* - \xi) + \frac{\pi}{2} \right) \gamma(\xi) d\xi = 2\pi A v \sin a \end{aligned}$$

Again substituting $\gamma(\xi)$ from equation (7) and integrating, there are obtained on the left side for the coefficients of A_1, A_2, A_3, A_4 , the following functions of λ and ξ^* .

$$F_1(\lambda, \xi^*) = \pi \left[\frac{\xi^{*5}}{16\lambda^5} + \frac{\xi^{*4}}{32\lambda^5} + \left(\frac{5}{16\lambda^5} - \frac{1}{8\lambda^3} \right) \xi^{*3} \right. \\ \left. + \left(\frac{15}{64\lambda^5} - \frac{3}{16\lambda^3} \right) \xi^{*2} + \left(\frac{15}{128\lambda^5} - \frac{3}{16\lambda^3} + \frac{1}{2\lambda} \right) \xi^* \right. \\ \left. + \left(\lambda + \frac{1}{4\lambda} - \frac{1}{64\lambda^3} + \frac{5}{256\lambda^5} + \frac{\pi}{2} \right) \right. \\ \left. + 0.280_{11} (\arcsin \xi^* + \sqrt{1 - \xi^{*2}}) \right]$$

$$F_2(\lambda, \xi^*) = \pi \left[\frac{\xi^{*5}}{32\lambda^5} + \left(\frac{5}{64\lambda^5} - \frac{1}{16\lambda^3} \right) \xi^{*3} \right. \\ \left. + \left(\lambda + \frac{1}{4\lambda} - \frac{3}{64\lambda^3} + \frac{5}{256\lambda^5} \right) \xi^* + \frac{\pi}{4} \right. \\ \left. + 0.140_{08} (\arcsin \xi^* + \xi^* \sqrt{1 - \xi^{*2}}) \right]$$

$$F_3(\lambda, \xi^*) = \pi \left[-\frac{5\xi^{*4}}{128\lambda^5} + \left(\lambda + \frac{3}{64\lambda^3} - \frac{5}{128\lambda^5} \right) \xi^{*2} \right. \\ \left. - \left(\frac{\lambda}{2} + \frac{1}{16\lambda} - \frac{1}{128\lambda^3} - \frac{5}{2048\lambda^5} \right) - 0.093_{37} (1 - \xi^{*2})^{3/2} \right]$$

$$F_4(\lambda, \xi^*) = \pi \left[\frac{\xi^{*5}}{128\lambda^5} + \left(\lambda - \frac{3}{64\lambda^3} + \frac{5}{128\lambda^5} \right) \xi^{*3} \right. \\ \left. - \left(\frac{\lambda}{2} - \frac{1}{16\lambda} + \frac{1}{128\lambda^3} - \frac{25}{2048\lambda^5} \right) \xi^* + \frac{\pi}{16} \right. \\ \left. + 0.035_{01} (\arcsin \xi^* - \xi^* \sqrt{1 - \xi^{*2}} (1 - 2\xi^{*2})) \right]$$

Again a definite value is taken for λ and for four points (here, too, the points chosen were $\xi_2^* = -\frac{1}{2}$, $\xi_2^* = 0$, $\xi_3^* = +\frac{1}{2}$, and $\xi_4^* = +1$) there are computed the 16 coefficient's of the system of equations

$\sum_{\mu=1}^4 F_{\mu}(\xi_{\mu}^*) A_{\mu} = 2\pi \lambda V \sin \alpha$ for $\mu = 1, 2, 3, 4$, from which the coefficients A_{μ} are determined. In this manner the A_{μ} for $\lambda = 6$ and $\lambda = 2$ are computed.

od. For $\lambda = 2$, this computation, strictly speaking, is at least for $\xi^* = 1$, not valid because the series into which the radical was developed is no longer convergent in the limiting case $\xi \rightarrow -1$.

Finally, equation (6) was also considered for the two limiting cases $A \rightarrow \infty$ and $A \rightarrow 0$. For the wing of infinite span, $b, \lambda \rightarrow \infty$, $E\left(\frac{\lambda}{\sqrt{\lambda^2 + (\xi^* - \xi)^2}}, \frac{\pi}{2}\right)$ becomes equal to 1 and the equation goes over into
$$\int_{-1}^{+1} \frac{1}{\xi^* - \xi} \gamma(\xi) d\xi =$$

$2\pi v \sin \alpha$. Substituting the above expression for $\gamma(\xi)$, there is easily recognized as a solution $\gamma(\xi) = 2V \sin \alpha \sqrt{\frac{1 - \xi}{1 + \xi}}$, which is the distribution given by the potential theory. Since as $A \rightarrow \infty$, the spanwise distribution becomes $\gamma(\eta) = \text{const}$, this solution satisfies the flow condition at each point of the surface. The same result is also obtained when in the method of solution for $\lambda > 2$, the $F_v(\lambda, \xi^*)$ are considered for very large λ and this system is computed. Then there is also obtained $A_1 = 2$, $A_2 = A_3 = A_4 = 0$. The lift coefficient will then be $c_a = \frac{\pi^2}{2} \sin \alpha$, and the moment coefficient $c_m = \frac{\pi^2}{2} \sin \alpha$, whereas, according to the two-dimensional potential theory, $c_a = 2\pi \sin \alpha$ and $c_m = \frac{\pi}{2} \sin \alpha$. This is again due to the fact that elliptical spanwise distribution was assumed for the rectangular wing; multiplying, subsequently, by $4/\pi$, the two results become identical. If an elliptical wing is considered and λ is made to approach infinity, there is immediately obtained $c_a = 2\pi \sin \alpha$ and $c_m = \frac{\pi}{4} \sin \alpha$ since the reference area for the coefficients is $\pi/4 b t$.

Of considerably greater difficulty is the limiting case of the wing with infinite chord $t \rightarrow \infty, \lambda \rightarrow 0$. Here the coordinates must be made nondimensional through the span instead of through the chord as heretofore: $x = \frac{b}{2} v, x^* = \frac{b}{2} v^*$. Equation (6) with $t \rightarrow \infty$ then goes over into:

$$\int_0^{\infty} \left\{ \frac{\sqrt{1+(v^*-v)^2}}{v^*-v} \mathbb{E} \left(\frac{1}{\sqrt{1+(v^*-v)^2}}, \frac{\pi}{2} \right) + \frac{\pi}{2} \right\} \gamma(v) dv = 2\pi v \sin \alpha$$

Again it was sought to find for $\gamma(v)$ a series of functions with undetermined coefficients which would then be determined through satisfying the integral equation at several points v^* . In this case, however, no series of functions could be found which at the leading edge $v \rightarrow 0$, increases as $1/\sqrt{v}$ and with $v \rightarrow \infty$, corresponding to the solution for $A = 1/4$, which decreases approximately as $1/v^3$. For this reason, only two following single functions were investigated: $\gamma_1(v) = \frac{A}{\sqrt{v + Bv^3}}$ and $\gamma_2(v) =$

$-\frac{C}{\sqrt{v + Dv^5}}$. Since again the integral could be evaluated

only graphically or numerically (on account of $0 \leq |v^*-v| < \infty$ a series development of the kernel could not be considered), it was necessary, before substituting, to assume B , and D , respectively, as fixed and then, by quadratures, set up $A(B, v^*)$ and $C(D, v^*)$, respectively, for several values of v^* . In order to limit the integration interval, it was again necessary to make another transformation:

$$u = \frac{1}{1+v}, \quad u^* = \frac{1}{1+v^*}$$

$$I_1(B; v^*, A) = \int_0^1 \left\{ \frac{\sqrt{1 + \left(\frac{u-u^*}{u u^*} \right)^2}}{\frac{u-u^*}{u u^*}} \mathbb{E} \left(\frac{1}{\sqrt{1 + \left(\frac{u-u^*}{u u^*} \right)^2}}, \frac{\pi}{2} \right) + \frac{\pi}{2} \right\} \frac{du}{u^3} \frac{A}{\sqrt{\frac{1}{u} - 1 + B \left(\frac{1}{u} - 1 \right)^3}}$$

Since the integrand again became singular at two points, namely, at $u \rightarrow u^*$ and $u \rightarrow 1$ ($u = 1$ corresponds to the leading edge, $u = 0$ to the trailing edge), the principal values had to be approximately determined by analytical methods. The entire laborious trial process, however, not

with little success as the effect of the various coefficients on the result was too difficult to estimate. As an approximation, it is possible to set at most $Y(v) \approx$

$$-\frac{1.12}{\sqrt{v} + 2.4 v^3}; \text{ for the range } 0.1 \leq v < \infty, \text{ the downwash}$$

error with respect to $v \sin \alpha$ then amounts to about 7 percent - this error, however, strongly increasing toward the leading edge ($v < 0.1$). The lift would then amount to $\Delta = 0.789 b^2 v^2 \sin \alpha$, and the center of pressure would lie at $s = 0.219 b$.

III. RESULTS

By the methods described, the chordwise lift distribution was computed for elliptic spanwise distribution for five aspect ratios, namely, $A = 1/4, 1/2, 1, 2$, and 6 , and graphically interpolated for arbitrary λ . The results are presented in figures 5 to 10 and are tabulated in the appendix. In figure 5 the coefficients for the circulation functions are plotted against A . A_1 increases monotonically and for large aspect ratio approaches 2 as the asymptotic value. The absolute values of the other coefficients increase up to a maximum at about $A = \frac{1}{2}$, then drop rapidly to zero; A_1 and A_3 are always positive, and A_2 and A_4 negative. The smaller A is, the less rapidly do the A_i converge, so that to obtain the same accuracy as for large aspect ratios, a longer series of functions for the circulation must be assumed. The curve $A_1 \sqrt{b/\lambda}$ shows the increase in the circulation in the neighborhood of the leading edge for constant span as a function of λ , since $\lim_{x \rightarrow 0} \gamma(x) = A_1 \sqrt{\frac{b}{\lambda}} \frac{1}{\sqrt{x}}$; here, too,

the maximum lies between $A = \frac{1}{2}$ and $\lambda = 1$. The value for $A = 0$ obviously is in error, from which fact it may be seen that the given approximation for $\gamma(v)$ does not correctly represent the behavior in the neighborhood of the leading edge. If the chord is held fixed and the span varied, A_1 itself gives the increase since $\lim_{x \rightarrow 0} \gamma(x) = A_1 \sqrt{t/x}$.

On figures 6 and 7 the circulation distribution $\gamma(\xi)/V \sin \alpha$ and the pressure difference between the

lower and upper sides of the plate referred to the dynamic pressure $\frac{\rho}{2} v^2 \sin \alpha = \frac{\pi}{2} \gamma(\xi)$ are plotted against the

chord. In figure 6 the abscissa refers to the chord, and in figure 7, to the span. In the first representation the limiting case $\lambda = 0$ coincides with the coordinate axes, so that the lift distributions for any aspect ratio lie between the axes and the limiting case $\lambda = \infty$. In the second representation the limiting case $A = \infty$ coincides with axis of ordinates. This method of plotting is particularly susceptible to error in the circulation distribution and shows that at $A = \frac{1}{2}$, a small error is to be assumed through inaccuracy of one of the graphical quadratures or the approximated principal value. Similarly, the limiting case $\lambda = 0$ appears as only a very rough approximation since intersection of the curves with each other is very improbable. It is seen, however, that for very small aspect ratio a further increase in the chord has only a small effect on the circulation distribution, either in the neighborhood of the leading edge or - owing to the strong decrease - farther toward the rear. This is seen especially clearly from the curve for $A/p b^2 v^2 \sin \alpha$ (fig. 8), which shows how the total lift increases when the span is held constant and the chord is varied.

On figures 9 and 10 the lift, drag, and moment coefficients are plotted as functions of A . They are computed from the values of A_1, A_2, A_3, A_4 as follows: The lift according to the Kutta-Joukowski theorem is:

$$A = \rho v \int_{-b/2}^{+b/2} dy \int_0^t \gamma(x, y) dx = \frac{\pi^2}{8} \rho v b t \left(A_1 + \frac{1}{2} A_3 + \frac{1}{8} A_4 \right)$$

from which $c_L = \frac{\pi^2}{4} \frac{1}{v} \left(A_1 + \frac{1}{2} A_3 + \frac{1}{8} A_4 \right)$. Similarly, the moment about the leading edge is

$$M = \rho v \int_{-b/2}^{+b/2} dy \int_0^t \gamma(x, y) x dx = \frac{\pi^2}{16} \rho v b t^2 \left(A_1 + A_2 + \frac{1}{4} A_3 + \frac{1}{4} A_4 \right)$$

and $c_M = \frac{\pi^2}{16} \frac{1}{v} \left(A_1 + A_2 + \frac{1}{4} A_3 + \frac{1}{4} A_4 \right)$ and finally the in-

duced drag is

$$W_1 = \rho \int_{-b/2}^{+b/2} dy \int_0^t \gamma(x, y) w(y) dx$$

where

$$dw(y) = \frac{1}{4\pi} \int_{-b/2}^{+b/2} \frac{\partial \gamma(x, y)}{\partial \bar{y}} dx \frac{d\bar{y}}{y - \bar{y}}$$

with

$$(x, y) = \frac{b}{2} \sqrt{1 - \left(\frac{y}{b/2}\right)^2} \sum_{v=1}^4 A_v \gamma_v(x)$$

we have

$$\frac{dw(y)}{dx} = - \frac{1}{2b} \sum_{v=1}^4 A_v \gamma_v(x) = \text{const}$$

on account of the elliptic spanwise distribution, so that $v_1 = \frac{\pi}{4\lambda} \left(A_1 + \frac{1}{2} A_2 + \frac{1}{8} A_4 \right)$ and $W_1 = \frac{\pi^3}{32} \rho t^2 \left(A_1 + \frac{1}{2} A_2 + \frac{1}{8} A_4 \right)^2$ and hence $c_{w1} = \frac{\pi^3}{16} \frac{1}{\lambda v^2} \left(A_1 + \frac{1}{2} A_2 + \frac{1}{8} A_4 \right)^2$.

Hence in this case also, $\frac{c_a^2}{c_{w1}} = \pi \lambda$. On account of the elliptic circulation distribution, the factor $v = \pi/4$; hence multiplying by $\frac{4}{\pi} v(\lambda)$ to take account of the v factor which increases with A , $(dc_a/dx)_0$ increases up to 2π as $\lambda \rightarrow \infty$. (The factor v was taken from the dissertation by A. Pets.) The induced drag coefficient increases with increasing A , has a maximum at about $\lambda = 2$ and then, since the drag remains finite while the area becomes larger, drops to zero. The position of the center of pressure is obtained from $s = (c_n/c_a) t$. This curve rapidly approaches the asymptote. At $\lambda = 3$, the deviation from the limiting value $s = 0.25 t$ is only 6 percent (fig. 10).

The agreement of the computation results by the vortex-filament method with those by the vortex-sheet method is surprisingly good. Even with two vortex filaments the deviations in the coefficients are small, whereas with four

vortex filaments the deviations become large only for very deep plates with $\lambda \leq 1$. (For $\lambda = 1$: $\Delta c_a/c_a \approx -0.4$ percent, $\Delta c_m/c_m \approx +3.4$ percent; for $\lambda = 1/2$: $\Delta c_a/c_a \approx -1.6$ percent, $\Delta c_m/c_m \approx +90$ percent.) The individual lift portions contributed by the four strips of the surface do not agree so well; for example:

Four vortex filaments			Vortex sheet		
Lift from 0 - 3t/16:	0.711	b t V sin α	0.665	b t V sin α	
3t/16 - 7t/16:	0.264	"	0.274	"	
7t/16 - 11t/16:	0.141	"	0.144	"	
11t/16 - t :	0.071	"	0.378	"	

The circulation of the foremost vortex always comes out too high, and that of the other vortices too low. In obtaining the moment this error is partially compensated by the consideration that too large lever arms are used for the three rear vortex filaments, which do not lie at the centers of gravity of AII, AIII, AIV.

With both methods the assumption of elliptic distribution over the span - which assumption makes possible the solution of the integral equation in the case of the vortex sheet - should be the greatest source of error. For this reason, too low lift coefficients are also obtained. The subsequent multiplication by the factor v does not appear to help sufficiently. According to the pressure distribution measurements of H. Winter which, however, are obtained for the square plate only, the distribution over the span at the loading edge is approximately elliptic, but farther toward the rear - almost up to the edge - it is constant, the edge disturbances which arise from the sharp edges of the investigated plate, however, not being taken into account.

, APPENDIX

I. 'Several vortex filaments: Two vortex filaments with elliptic circulation distribution over the span at $x = t/8$ and $x = 5t/8$.

$\lambda = \frac{1}{2}$	$A_I = 0.3571 \text{ } \beta t V \sin a$	$c_a = 0.770 \sin a$	$s = 0.161 t$
	$A_{II} = 0.0277 \text{ } \beta t V \sin a$	$c_m = 0.124 \sin a$	
$\lambda = 1$	$A_I = 0.6132 \text{ } \beta t V \sin a$	$c_a = 1.436 \sin a$	$s = 0.198 t$
	$A_{II} = 0.1050 \text{ } \beta t V \sin a$	$c_m = 0.285 \sin a$	
$\lambda = 2$	$A_I = 0.9410 \text{ } \beta t V \sin a$	$c_a = 2.269 \sin a$	$s = 0.228 t$
	$A_{II} = 0.2434 \text{ } \beta t V \sin a$	$c_m = 0.540 \sin a$	
$\lambda = 6$	$A_I = 1.4280 \text{ } \beta t V \sin a$	$c_a = 3.767 \sin a$	$s = 0.246 t$
	$A_{II} = 0.4557 \text{ } \beta t V \sin a$	$c_m = 0.923 \sin a$	

Four vortex filaments with elliptic circulation distribution over the span at $x = t/16, 5t/16, 9t/16$, and $13t/16$.

Vortex sheet

$\lambda = \frac{1}{2}$	$A_I = 0.5080 \text{ } \beta t V \sin a$	(0.2979)	$c_a = 0.772 \sin a$
	$A_{II} = 0.0557$	" (0.0724)	$c_w = 0.379 \sin^2 a$
	$A_{III} = 0.0165$	" (0.0154)	$c_m = 0.101 \sin a$
	$A_{IV} = 0.0058$	" (0.0067)	$s = 0.131 t$
$\lambda = 1$	$A_I = 0.4876 \text{ } \beta t V \sin a$	(0.4838)	$c_a = 1.441 \sin a$
	$A_{II} = 0.1433$	" (0.1470)	$c_w = 0.661 \sin^2 a$
	$A_{III} = 0.0623$	" (0.0627)	$c_m = 0.265 \sin a$
	$A_{IV} = 0.0273$	" (0.0299)	$s = 0.184 t$
$\lambda = 2$	$A_I = 0.7111 \text{ } \beta t V \sin a$	(0.6852)	$c_a = 2.374 \sin a$
	$A_{II} = 0.2644$	" (0.2739)	$c_w = 0.897 \sin^2 a$
	$A_{III} = 0.1405$	" (0.1442)	$c_m = 0.528 \sin a$
	$A_{IV} = 0.0710$	" (0.0782)	$s = 0.222 t$

Vortex sheet

$$\begin{aligned}
 \lambda = 6 \quad A_I &= 1.0480 \, b \sqrt{V} \sin \alpha & (1.0068) & \quad c_n = 3.770 \sin \alpha \\
 A_{II} &= 0.4385 & " & \quad (0.4425) \quad c_w = 0.754 \sin^2 \alpha \\
 A_{III} &= 0.2576 & " & \quad (0.2525) \quad c_n = 0.923 \sin \alpha \\
 A_{IV} &= 0.1406 & " & \quad (0.1465) \quad a = 0.245 \, t
 \end{aligned}$$

II Vortex surface: Examples for $\lambda < 2$

$$\begin{aligned}
 \lambda = \frac{1}{2} \quad J_1 &= 6.3138 \quad J_2 = 0.6725 \quad J_3 = -0.7284 \quad J_4 = 0.5566 \\
 J_5 &= 8.2523 \quad J_6 = 2.4674 \quad J_7 = -1.1575 \quad J_8 = 0.6169 \\
 J_9 &= 9.4427 \quad J_{10} = 4.0623 \quad J_{11} = -0.7284 \quad J_{12} = 0.6772 \\
 J_{13} &= 10.0592 \quad J_{14} = 5.2067 \quad J_{15} = 0.2581 \quad J_{16} = 1.4606 \\
 A_1 &= 0.3435 \, v \sin \alpha \quad c_n = 0.3839 \sin \alpha \quad A_1 / \sqrt{\lambda} = 0.687 \, v \sin \alpha \\
 A_2 &= -0.3307 & " & \quad c_w = 0.126 \sin^2 \alpha \quad \text{total lift:} \\
 A_3 &= 0.2994 & " & \quad c_n = 0.0287 \sin \alpha \quad A = 0.7778 \, \rho \, b^2 \, v \\
 A_4 &= -0.1642 & " & \quad s = 0.0739 \, t
 \end{aligned}$$

$$\begin{aligned}
 \lambda = \frac{1}{2} \quad J_1 &= 6.8189 \quad J_2 = 0.6345 \quad J_3 = -1.0013 \quad J_4 = 0.6956 \\
 J_5 &= 8.6508 \quad J_6 = 2.4674 \quad J_7 = -1.5644 \quad J_8 = 0.6157 \\
 J_9 &= 9.7617 \quad J_{10} = 4.2703 \quad J_{11} = -1.0013 \quad J_{12} = 0.5381 \\
 J_{13} &= 10.3816 \quad J_{14} = 5.8817 \quad J_{15} = 0.6725 \quad J_{16} = -1.7546 \\
 A_1 &= 0.5793 \, v \sin \alpha \quad c_n = 0.7846 \sin \alpha \quad A_1 / \sqrt{\lambda} = 0.819 \, v \sin \alpha \\
 A_2 &= -0.4802 & " & \quad c_w = 0.3919 \sin^2 \alpha \quad A = 0.7846 \, \rho \, b^2 \, v^2 \\
 A_3 &= 0.3710 & " & \quad c_n = 0.0922 \sin \alpha \\
 A_4 &= -0.1697 & " & \quad s = 0.1175 \, t
 \end{aligned}$$

$$\begin{aligned}
 \lambda = 1 \quad J_1 &= 8.1785 \quad J_2 = 0.1265 \quad J_3 = -1.1401 \quad J_4 = 0.8755 \\
 J_5 &= 9.6696 \quad J_6 = 2.4674 \quad J_7 = -1.9864 \quad J_8 = -0.6169 \\
 J_9 &= 10.6560 \quad J_{10} = 4.8083 \quad J_{11} = -1.1401 \quad J_{12} = 0.3583 \\
 J_{13} &= 11.3206 \quad J_{14} = 7.0036 \quad J_{15} = 1.3577 \quad J_{16} = 2.4958 \\
 A_1 &= 0.8182 \text{ V sin } \alpha \quad c_R = 1.4456 \text{ sin } \alpha \quad A_1 / \sqrt{\lambda} = 0.818 \text{ V sin } \alpha \\
 A_2 &= -0.4424 \quad " \quad c_V = 0.5562 \text{ sin}^2 \alpha \quad A = 0.7233 \text{ p } b^2 v^2 \\
 A_3 &= 0.2440 \quad " \quad c_M = 0.2563 \text{ sin } \alpha \\
 A_4 &= -0.0852 \quad " \quad s = 0.1771 \text{ t}
 \end{aligned}$$

Examples for $\lambda \geq 2$

$$\begin{aligned}
 \lambda=2 \quad F_1 &= 3.6683\pi \quad F_2 = -0.4078\pi \quad F_3 = -0.5899\pi \quad F_4 = 0.4204\pi \\
 F_5 &= 3.9707\pi \quad F_6 = 0.7854\pi \quad F_7 = -1.1236\pi \quad F_8 = 0.1964\pi \\
 F_9 &= 4.1905\pi \quad F_{10} = 1.9786\pi \quad F_{11} = -0.5898\pi \quad F_{12} = -0.0277\pi \\
 F_{13} &= 4.3408\pi \quad F_{14} = 3.1208\pi \quad F_{15} = 0.9732\pi \quad F_{16} = 1.2815\pi \\
 A_1 &= 1.0790 \text{ V sin } \alpha \quad c_R = 2.3629 \text{ sin } \alpha \quad A_1 / \sqrt{\lambda} = 0.763 \text{ V sin } \alpha \\
 A_2 &= -0.2389 \quad " \quad c_V = 0.8886 \text{ sin}^2 \alpha \quad A = 0.5937 \text{ p } b^2 v^2 \\
 A_3 &= 0.0834 \quad " \quad c_M = 0.5288 \text{ sin } \alpha \\
 A_4 &= -0.0149 \quad " \quad s = 0.2238 \text{ t} \\
 \lambda=6 \quad F_1 &= 7.6668\pi \quad F_2 = -2.3693\pi \quad F_3 = -1.5710\pi \quad F_4 = 0.9304\pi \\
 F_5 &= 7.8924\pi \quad F_6 = 0.7854\pi \quad F_7 = -3.1037\pi \quad F_8 = 0.1964\pi \\
 F_9 &= 8.0425\pi \quad F_{10} = 3.9401\pi \quad F_{11} = -1.5710\pi \quad F_{12} = -0.5377\pi \\
 F_{13} &= 8.1334\pi \quad F_{14} = 7.0466\pi \quad F_{15} = 2.9898\pi \quad F_{16} = 3.2617\pi
 \end{aligned}$$

$$\begin{aligned}
 A_1 &= 1.5449 \, v \sin \alpha \quad c_a = 3.6946 \sin \alpha \quad A_1 / \sqrt{\lambda} = 0.631 \, v \sin \alpha \\
 A_2 &= -0.09344 \quad " \quad c_w = 0.7242 \sin^2 \alpha \quad A = 0.3079 \, \rho \, b^2 \, v^2 \\
 A_3 &= 0.03808 \quad " \quad c_m = 0.9002 \sin \alpha \\
 A_4 &= -0.00530 \quad " \quad s = 0.2437 \, t
 \end{aligned}$$

$$\lambda = \infty \quad A_1 = 2V \sin \alpha \quad c_a = \frac{\pi^2}{2} \sin \alpha \text{ instead of } c_a = 2\pi \sin \alpha$$

$$A_2 = A_3 = A_4 = 0 \quad c_m = \frac{\pi^2}{8} \sin \alpha \quad " \quad " \quad c_m = \frac{\pi}{2} \sin \alpha$$

$$s = 0.25 \, t$$

Translation by S. Reiss,
 National Advisory Committee
 for Aeronautics.

REFERENCES

1. Prandtl, L.: Tragflächentheorie I und II. Göttinger Nachrichten 1918-1919.
2. Betz, A.: Beiträge zur Tragflügeltheorie mit besonderer Berücksichtigung des einfachen rechteckigen Flügels. Diss. Göttingen, 1919.
3. Trefftz, E.: Prandtl'sche Tragflächen- und Propeller-Theorie. Zeitschrift für angewandte Mathematik und Mechanik. Bd. 1. 1921, S. 203.
4. Pirubaum, W.: Die tragende Wirbelfläche als Hilfsmittel zur Behandlung des ebenen Problems der Tragflügeltheorie. Zeitschrift für angewandte Mathematik und Mechanik. Bd. 3, 1923. S. 290.
5. Blenk, H.: Der Eindecker als tragende Wirbelfläche. Zeitschrift für angewandte Mathematik und Mechanik, Bd. 5, 1925, S. 36.
6. Prandtl, L.: Beitrag zur Theorie der tragenden Fläche. Zeitschrift für angewandte Mathematik und Mechanik, Bd. 15, 1936, S. 360.
7. Kinner, W.: Die kreisförmige Tragfläche auf potential-theoretischer Grundlage. Ingenieur-Archiv, Bd. 8, 1937. S. 47.
8. Winter, H.: Flow Phenomena on Platos and Airfoils of Short Span, T.M. No. 798, NACA, 1936.

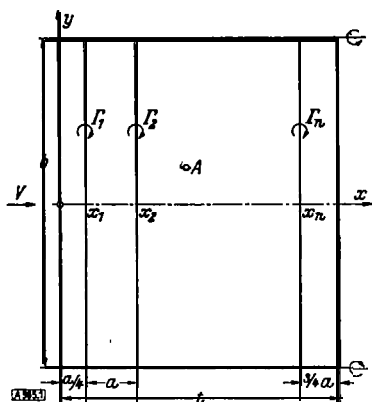


Figure 1.

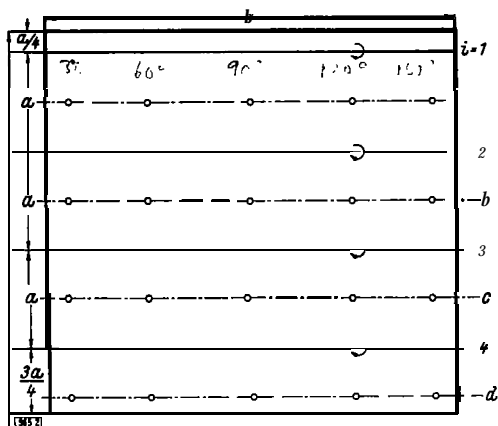
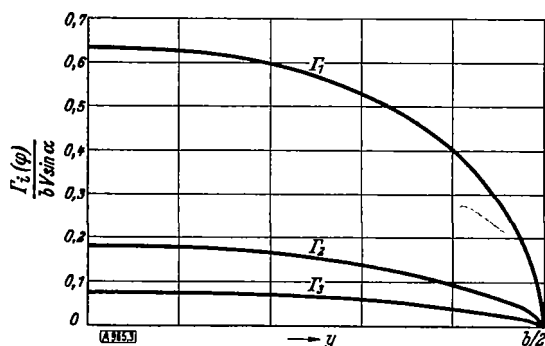
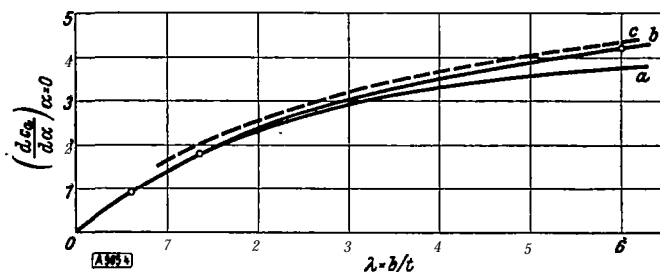
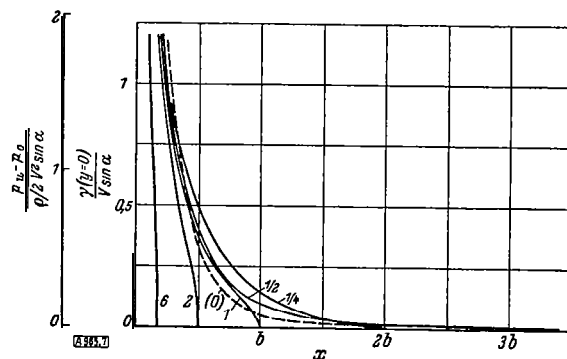
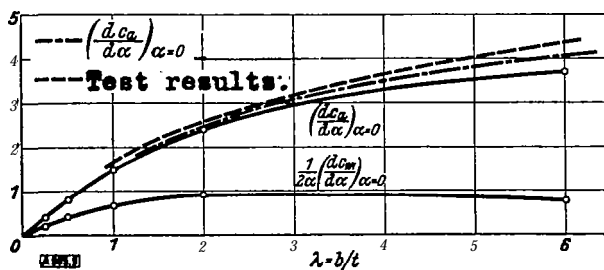


Figure 2.

Figure 9.- Lift and drag coefficients as functions of λ .Figure 4.- Lift distribution as a function of λ for a vortex filament, a, $\Gamma(\varphi) = \Gamma \sin \varphi$; b, $\Gamma(\varphi) = \Gamma \sin \varphi (1 + a_1 \sin \varphi)$; c, test result of Winter.Figure 7.- Circulation distribution over the chord; $b = \text{const.}$ Figure 3.- Circulation distribution of the forward three vortex filaments at $x = t/16, 5t/16, 9t/16; \lambda = 1$.

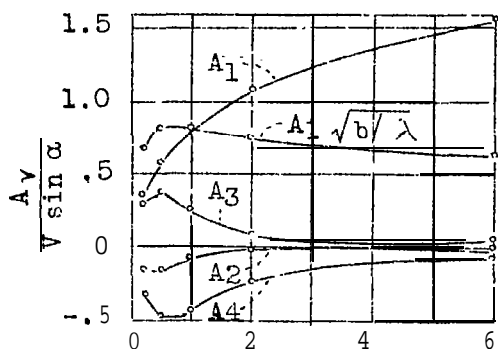


Figure 5.- Coefficients of circulation functions for various aspect ratios.

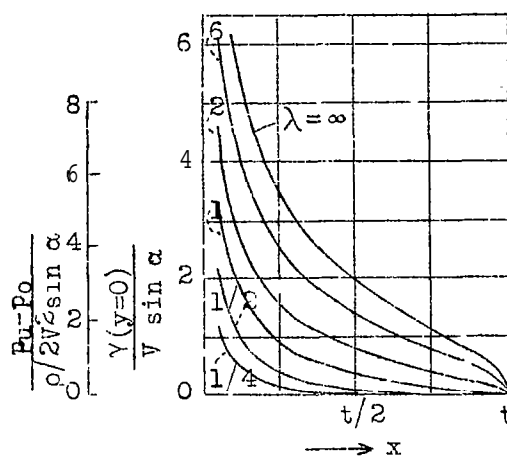


Figure 6.- Circulation distribution over the chord; $t = \text{const}$,

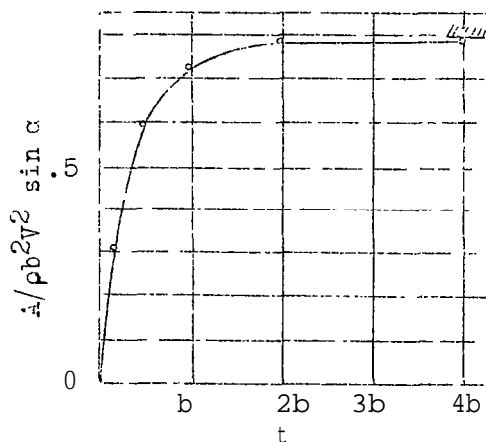


Figure 8.- Total lift as a function of the chord.

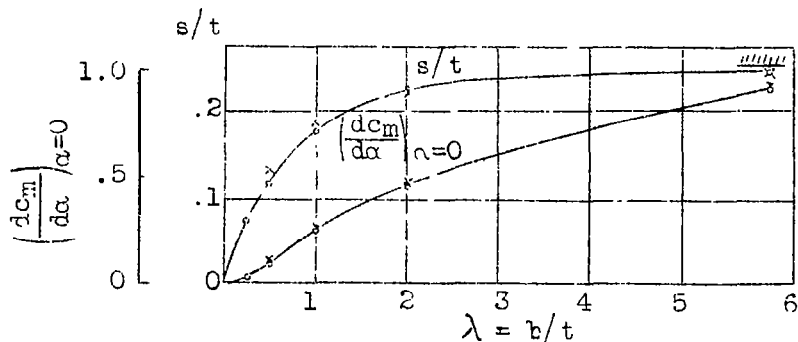


Figure 10.- Moment coefficient and distance of center of pressure from leading edge as functions of λ . (points x computed with four vortex lines).

NASA Technical Library



3 1176 01440 7135